Molecular-Weight Distribution Attainable in a Batch Free-Radical Polymerization

Kee-Youn Yoo and Hyun-Ku Rhee
School of Chemical Engineering and Institute of Chemical Processes, Seoul National University, Seoul 151-742, Korea

The attainable values of molecular-weight distribution (MWD) specified by the degree of polymerization and the polydispersity in a batch free-radical polymerization reactor are described. The two-step method based on the quadratic profile of the instantaneous degree of polymerization is used to obtain the recipe producing the polymer with the desired MWD specification. The analytic solution for the quadratic profile is derived and analyzed in order to estimate the attainable MWD given the constraints on the range of the instantaneous degree of polymerization. The entire computational procedure is intelligently organized, and thus the actual computational load is very low compared to the conventional optimization scheme. The MWD attainable under a specific operating condition with constraints in a batch styrene polymerization reactor is visualized and various reactor temperature trajectories that would produce the desired polymer product are calculated. The ability to predict the attainable MWD allows an engineer to easily design the recipes that would meet the desired MWD specification.

Introduction

The batch polymerization process is widely used in industries for its availability and flexibility in operation. In a batch free-radical polymerization process, a typical operation task involves the manipulation of reactant concentrations, reactor temperature, and other adjustable variables to achieve desired targets for conversion, molecular weight, and residual impurities. These are actually indirect specifications of the end-use and processing properties needed by the customer. Many end-use properties are correlated with the average molecular weight (MW) and molecular weight distribution (MWD), including tensile strength, impact strength, fatigue life, and melting point (Nunes et al., 1982). Molecular weight also affects the processing properties (Tadmor and Gogos, 1979).

Hence, operating a polymerization process to achieve a specified average MW and MWD is highly desired. However, control of MW and MWD is a very difficult task, with on-line measurement being the primary obstacle. Without measurement, feedback control of MW and MWD is not possible. Thus the polymerization process is operated according to a predetermined recipe (such as reactor temperature trajectory or initiator supply policy) that has been obtained to produce a polymer with the desired properties. In industrial practice, the recipe is usually determined by trial-and-error experience. A less common industrial approach for determining the recipe is to use polymerization models.

Many researchers have used the optimal-control theory in order to determine a recipe that minimizes the reaction time and produces the polymer with the desired average MWs in a batch reactor (Hicks et al., 1969; Sacks et al., 1972; Chen and Jeng, 1978; Thomas and Kiparissides, 1984; Ponnuswamy et al., 1987; Ahn et al., 1998). The derived optimization problem is, however, nonconvex and leads to many difficulties against implementation; that is, feasibility, optimality, and computation. Also, these calculations usually require simplification of the reaction kinetics involved.

Takamatsu et al. (1988) proposed the two-step method based on the instantaneous degree of polymerization needed to determine the temperature trajectory that would produce the desired average MWs in a batch suspension styrene polymerization reactor. This method transforms the average molecular-weight control problem into a one-parameter searching problem. Thus, the time-consuming complex computation can be avoided, and the criterion to judge whether or not the reactor temperature trajectory is feasible in a given reactor system can be easily derived (Chang and Lai, 1992).

Correspondence concerning this article should be addressed to H.-K. Rhee.

In polymerization processes, the preferred operating condition should take into account the end-use properties, ease of processing, and operating costs. Hence, it is necessary to evaluate which specifications can be realized under a given operating condition. Recently, we implemented the on-line two-step method that repeatedly uses a numerical algorithm developed for an open-loop scheme at each time step (Yoo et al., 1998). For the on-line scheme, it is also necessary to judge the existence of the feasible solution at each time step and calculate the recipe as fast as possible. The conventional optimization scheme, however, is very slow to meet these objectives.

In this study, we examine what specifications for average MWs are realizable in a batch polymerization reactor when the two-step method is applied. At first, we formulate the equations for the first step in dimensionless form and derive simple analytic solutions (the quadratic profiles for the instantaneous degree of polymerization) that would give rise to the desired average MWs. We then investigate the range of feasible average MWs attainable by the two-step method based on the quadratic solutions for both unconstrained and constrained cases. Finally, we perform the simulation study for styrene polymerization in a batch reactor, and discuss various operational strategies to produce polymer with the desired average molecular weights.

Batch Polymerization Reactor Model

In this section, we describe a batch-reactor model for the solution polymerization. The reaction kinetics is assumed to follow the free-radical polymerization mechanism, including chain transfer reactions to both solvent and monomer. The general free-radical polymerization mechanism is summarized in Table 1. The method of moments is adopted to calculate the number average molecular weight (Mn) and the weight average molecular weight (Mw). The definitions of the moments are as follows:

$$G_k = \sum_{n=1}^{\infty} n^k R_n(t) \qquad \text{and} \qquad F_k = \sum_{n=1}^{\infty} n^k P_n(t), \qquad k = 0, 1, 2. \quad (1)$$

The dynamic behavior of the reactor is described by the equations reported in Table 2. As the monomer is converted to polymer, the density of the reaction mixture increases, and thus the volume V of the reactor contents shrinks. Therefore, we use the appropriate density correlation to take into account the volume change of the reaction mixture; that is,

$$V_m = (MV)\frac{W_m}{\rho_m}, \qquad V_s = (SV)\frac{W_s}{\rho_s},$$

$$V_p = [M(0)V(0) - MV]\frac{W_m}{\rho_p}. \quad (2)$$

Table 1. Free-Radical Polymerization Mechanism

Initiation	$I \xrightarrow{k_d} 2\varphi\cdot$
	$\varphi\cdot + M \xrightarrow{k_i} R_1$
Propagation	$R_1 + M \xrightarrow{k_p} R_2$
	$R_j + M \xrightarrow{k_p} R_{j+1}$
Termination by combination	$R_i + R_j \xrightarrow{k_{tc}} P_{i+j}$
Termination by disproportionation	$R_i + R_j \xrightarrow{k_{td}} P_i + P_j$
Chain transfer to monomer	$R_i + M \xrightarrow{k_{trm}} P_i + R_1$
Chain transfer to solvent	$R_i + S \xrightarrow{k_{trs}} P_i + R_1$

Table 2. Balance Equations for the Batch Reactor

$$\frac{1}{V}\frac{d(IV)}{dt} = -k_d I$$

$$\frac{1}{V}\frac{d(MV)}{dt} = -2fk_d I - k_p M G_0 - k_{trm} M G_0$$

$$\frac{1}{V}\frac{d(SV)}{dt} = -k_{trs} S G_0$$

$$\frac{1}{V}\frac{d(G_0V)}{dt} = 2fk_d I - k_t G_0^2$$

$$\frac{1}{V}\frac{d(G_1V)}{dt} = 2fk_d I + k_p M G_0 - k_t G_0 G_1 + (k_{trm} M + k_{trs} S)(G_0 - G_1)$$

$$\frac{1}{V}\frac{d(G_2V)}{dt} = 2fk_d I + k_p M(G_0 + 2G_1) - k_t G_0 G_2 + (k_{trm} M + k_{trs} S)(G_0 - G_2)$$

$$\frac{1}{V}\frac{d(F_0V)}{dt} = \frac{1}{2}(k_t + k_{td})G_0^2 + (k_{trm} M + k_{trs} S)G_0$$

$$\frac{1}{V}\frac{d(F_1V)}{dt} = k_t G_0 G_1 + (k_{trm} M + k_{trs} S)G_1$$

$$\frac{1}{V}\frac{d(F_2V)}{dt} = k_{tc}(G_0 G_2 + G_1^2) + k_{td} G_0 G_2 + (k_{trm} M + k_{trs} S)G_2$$

In this work, we apply this batch polymerization reactor model to the styrene polymerization system. We also contain the empirical gel effect correlation suggested by Hamer et al. (1981) in the reactor model. The physical properties and kinetic parameters were taken from the literature and are listed in Table 3. However, the chain transfer rate constants were determined by applying the parameter-estimation technique to the experimental data.

Two-Step Method for the MWD Control in a Batch Reactor

In most cases, MWD is fairly well described by the number average molecular weight Mn and the polydispersity P. Therefore, the MWD control problem in a batch reactor boils down to that of searching an operating condition to produce the polymer with the prescribed number average degree of polymerization Y^* and the prescribed polydispersity P^* at the desired conversion level X^*. At time t, the number average degree of polymerization $Y(t)$ and the polydispersity $P(t)$ are expressed as

$$Y(t) = \frac{F_1(t) + G_1(t)}{F_0(t) + G_0(t)},$$

$$P(t) = \frac{\{F_0(t) + G_0(t)\}\{F_2(t) + G_2(t)\}}{\{F_1(t) + G_1(t)\}^2} \quad (3)$$

Table 3. Parameters Used in the Model for Styrene Polymerization

Physical Properties		
ρ_m [g/L]	$924.0 - 0.981 \times (T - 273.15)$	Schuler and Suzhen (1985)
ρ_s [g/L]	$885.5 - 0.955 \times (T - 273.15)$	Schuler and Suzhen (1985)
ρ_p [g/L]	$1084.0 - 0.605 \times (T - 273.15)$	Takamatsu et al. (1988)
Rate Constants		
k_d [s^{-1}]	$1.58 \times 10^{15} \exp(-30780/RT)$	Duerksen et al. (1967)
k_p [L/mol/s]	$1.051 \times 10^{7} \exp(-7064/RT)$	Duerksen et al. (1967)
k_{t0} [L/mol/s]	$1.255 \times 10^{9} \exp(-1680/RT)$	Duerksen et al. (1967)
k_{trm} [L/mol/s]	$1.186 \times 10^{7} \exp(-11767/RT)$	Estimated
k_{trs} [L/mol/s]	$3.148 \times 10^{9} \exp(-16264/RT)$	Estimated
Gel Effect Correlation		
$g_t(X,T) = \dfrac{k_t}{k_{t0}} = \exp[-2(Ax + Bx^2 + Cx^3)]$, $x = X(1 - f_s)$, f_s = solvent fraction where $A = 2.57 - 5.05 \times 10^{-3} T$ $B = 9.56 - 1.76 \times 10^{-2} T$ $C = -3.03 + 7.85 \times 10^{-3} T$		

and the conversion $X(t)$ in a batch reactor is given by

$$X(t) = \frac{V(0)M(0) - V(t)M(t)}{V(0)M(0)} = \frac{\{F_1(t) + G_1(t)\}V(t)}{V(0)M(0)}, \tag{4}$$

where the total amount of polymer produced is calculated from the monomer material balance. If $X(t)$, $Y(t)$, and $P(t)$ in Eqs. 3 and 4 are replaced by X^*, Y^*, and P^*, respectively, the desired values of the moments of polymer concentrations are obtained as follows:

$$\begin{aligned} H_0^* &= \{F_0(t) + G_0(t)\}V(t) = V(0)M(0)X^*/Y^* \\ H_1^* &= \{F_1(t) + G_1(t)\}V(t) = V(0)M(0)X^* \\ H_2^* &= \{F_2(t) + G_2(t)\}V(t) = V(0)M(0)X^*Y^*P^*. \end{aligned} \tag{5}$$

Therefore, given the control objectives X^*, Y^*, and P^* and the initial reactor condition, the MWD control problem is equivalent to that of searching an operating condition to produce the polymer with H_0^*, H_1^*, and H_2^*.

It is then necessary to monitor the relations among H_0, H_1, and H_2 during a batch reactor operation. For this purpose, the instantaneous degree of polymerization y and the instantaneous polydispersity p are defined as

$$y = \frac{dH_1}{dt} \bigg/ \frac{dH_0}{dt}, \quad p = \left\{\frac{dH_0}{dt}\right\}\left\{\frac{dH_2}{dt}\right\} \bigg/ \left\{\frac{dH_1}{dt}\right\}^2. \tag{6}$$

These equations can be recast in the form $dH_1/dH_2 = y$ and $dH_2/dH_0 = py^2$. This implies that both H_1 and H_2 may be expressed in terms of H_0, so integration of Eq. 6 from 0 to H_0^* gives the following equations:

$$H_1^* = \int_0^{H_0^*} y(H_0)\, dH_0 \tag{7}$$

$$H_2^* = \int_0^{H_0^*} p(H_0)\, y^2(H_0)\, dH_0. \tag{8}$$

These equations must always be satisfied to obtain the polymer product with the desired properties. For the simplicity of calculation, $p(H_0)$ is assumed to be constant during a batch. This assumption has been found reasonable by the simulation results of the present study. Furthermore, one can put Eqs. 7 and 8 into dimensionless form:

$$1 = \int_0^1 \left(\frac{y}{Y^*}\right) d\left(\frac{H_0}{H_0^*}\right) \tag{9}$$

$$\frac{P^*}{p} = \int_0^1 \left(\frac{y}{Y^*}\right)^2 d\left(\frac{H_0}{H_0^*}\right), \tag{10}$$

in which the following relationship should be satisfied:

$$\frac{P^*}{p} \geq 1. \tag{11}$$

Equation 11 implies that the attainable minimum polydispersity is equal to p.

Here, we can separate the MWD control problem into two steps: the first step is to determine $y^*(H_0)$ satisfying Eqs. 9 and 10, while the second step is to explore the operating conditions forcing $y(H_0)$ to $y^*(H_0)$ determined in the first step.

First step based on the quadratic expression for y

Takamatsu et al. (1988) used three different types of expression for $y(H_0)$: (1) a rectangular type; (2) a quadratic type; and (3) a mixed type of zero and first-order polynomial. Here, we consider the quadratic expression for $y(H_0)$ to execute the two-step method: $y(H_0) = y(0) + a_1 H_0 + a_2 H_0^2$, where $y(0)$ is calculated by using the initial reactor condition. In general, the quadratic expression is preferred to other ones because of the fact that the profile of y is smooth and the attainable MWD is sufficiently extensive. Various expressions for $y(H_0)$, however, may be chosen considering the reactor operability.

The quadratic expression for $y(H_0)$ can be inserted into Eqs. 9 and 10 to determine a_1 and a_2, respectively. The resulting $y(H_0)$ trajectories are derived in dimensionless form as follows:

$$\frac{y^*(H_0)}{Y^*}=[1+\beta]-\frac{3}{2}[3\beta+5D]\left(\frac{H_0}{H_0^*}\right)+\frac{15}{4}[\beta+3D]\left(\frac{H_0}{H_0^*}\right)^2,$$

$$D=\pm\sqrt{\frac{1}{15}(8\alpha-\beta^2)} \tag{12}$$

where

$$\alpha=\frac{P^*}{p}-1 \quad \text{and} \quad \beta=\frac{y(0)}{Y^*}-1. \tag{13}$$

Here α is the dimensionless parameter related to the relative ratio of the desired polydispersity to the attainable minimum polydispersity, and β is the dimensionless quantity associated with the initial reactor condition. For the sake of convenience, we call Eq. 12 the quadratic constitutive equation (QCE). The desired polymer product is to be obtained if the instantaneous degree of polymerization y tracks one of the two trajectories given by QCE during the course of polymerization. It is important to know that these QCEs for $D \geq 0$ and for $D < 0$ are only the subset of $y^*(H_0)$ trajectories satisfying Eqs. 9 and 10.

Second step: Calculation of the recipe for the reactor operation

In the second step, the reactor operating condition that realizes the y^* profile determined in the first step should be calculated based on the polymerization reactor model. Using the conservation equations for the moments of the living and dead polymer concentrations, the instantaneous degree of polymerization y is derived as follows:

$$y=\frac{dH_1}{dH_0}=\frac{2fk_dI+k_pMG_0+(k_{trm}M+k_{trs}S)G_0}{2fk_dI-0.5k_{tc}G_0^2+(k_{trm}M+k_{trs}S)G_0}. \tag{14}$$

Here, we assume that the reactor temperature is primarily used to control the MWD with the given initiator amount and solvent fraction. Therefore, one can calculate the right-hand side of Eq. 14 for a given temperature and indeed determine the temperature trajectory that makes the time profile $y(t)$ of Eq. 14 equal to the $y^*(H_0)$ profile obtained in the first step.

In actual calculation, the mass-balance equations for I, M, S, and G_0 need to be integrated simultaneously, and the following equation is used to map the $y^*(H_0)$ profile into the corresponding time profile $y(t)$:

$$\frac{dt}{dH_0}=\frac{V}{2fk_dI-1/2k_{tc}G_0^2+(k_{trm}M+k_{trs}S)G_0}. \tag{15}$$

This procedure will lead to the actual operating policy required.

MWD Attainable by the Two-step Method Based on QCEs

MWD attainable by QCEs without constraints on the range of y

Let us first explore the MWD attainable by QCEs without constraints on the range of y. In this case, the attainable MWD can be easily estimated by investigating the physically realizable pairs of (α, β) in QCEs. The feasible value of α is closely related to the attainable polydispersity by Eq. 13; that is, if the larger value of α is feasible, the polymer product with a larger polydispersity can be obtained.

The physically realizable pairs of (α, β) can be determined by requiring in Eq. 12 that D be real and y^* be positive; that is,

$$\alpha \geq \frac{1}{8}\beta^2 \quad \text{and} \quad \frac{y^*}{Y^*} > 0. \tag{16}$$

Figure 1 shows the regions of (α, β) corresponding to the

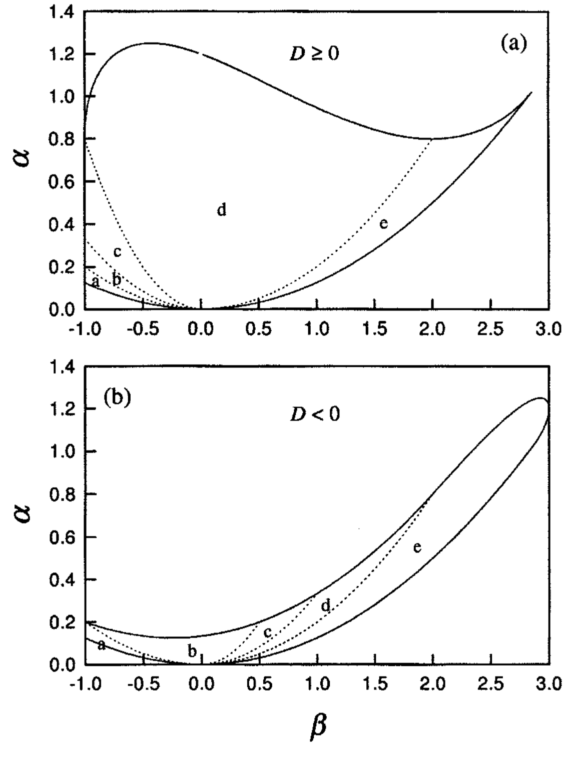

Figure 1. Physically realizable regions for the pairs of (α, β) attainable by the two-step method based on QCEs.

$\alpha(=P^*/p-1)$ is related to the ratio of the desired polydispersity P^* to the attainable minimum polydispersity p, and β $(=y(0)/Y^*-1)$ is related to the ratio of the initial instantaneous degree of polyermization $y(0)$ to the desired degree of polymerization Y^*. The individual regions of each caption can be represented by the following expressions: (a) a: $(1/8\beta^2 \leq \alpha < 1/5\beta^2)\wedge(\beta \leq 0)$, b: $(1/5\beta^2 \leq \alpha < 1/3\beta^2)\wedge(\beta \leq 0)$, c: $(1/3\beta^2 \leq \alpha < 4/5\beta^2)\wedge(\beta \leq 0)$, d: $\{(4/5\beta^2 \leq \alpha)\wedge(\beta \leq 0)\}\vee\{(1/5\beta^2 \leq \alpha)\wedge(\beta > 0)\}$, e: $(1/8\beta^2 \leq \alpha < 1/5\beta^2)\wedge(\beta > 0)$. (b) a: $(1/8\beta^2 \leq \alpha < 1/5\beta^2)\wedge(\beta \leq 0)$, b: $\{(4/5\beta^2 \leq \alpha)\wedge(\beta > 0)\}\vee\{(1/5\beta^2 \leq \alpha)\wedge(\beta \leq 0)\}$, c: $(1/3\beta^2 \leq \alpha < 4/5\beta^2)\wedge(\beta > 0)$, d: $\{(1/5\ \beta^2 \leq \alpha < 1/3\beta^2)\wedge(\beta > 0)$, e: $(1/8\beta^2 \leq \alpha < 1/5\beta^2)\wedge(\beta > 0)$.

physically realizable QCEs satisfying Eq. 16. For the case of QCE for $D \geq 0$, the upper bound of α in Figure 1a is given by

$$\alpha_u = \frac{1}{10}\left[\beta^2 - \beta + 6 + (2-\beta)\sqrt{3(3-\beta)(1+\beta)}\right] \quad \text{for} \quad -1 < \beta < \frac{20}{7}, \tag{17}$$

along which the minimum value of y is equal to zero. The maximum value of α_u is obtained as

$$\alpha_{u,M} = \frac{5}{4} \quad \text{at} \quad \beta = \frac{5-3\sqrt{5}}{4}. \tag{18}$$

Thus the maximum polydispersity attainable is equal to $9p/4$. On the other hand, the lower bound of α in Figure 1a is given by

$$\alpha_l = \frac{1}{8}\beta^2 \quad \text{for} \quad -1 < \beta < \frac{20}{7}, \tag{19}$$

along which the value of D remains as zero.

Now it is to be noticed that one can think of five different patterns for the QCE profile for $D \geq 0$ as depicted in Figure 2a. Corresponding to each of these patterns, one obtains a subregion marked within the feasible region of Figure 1a.

In the same manner, one can examine the feasible MWD based on QCE for $D < 0$. The upper bound of α in Figure 1b is derived to give

$$\alpha_u = \begin{cases} \dfrac{1}{15}(2\beta^2 + \beta + 2) & \text{for} -1 < \beta < 2 \\ \dfrac{1}{10}\left[\beta^2 - \beta + 6 + (\beta - 2)\sqrt{3(3-\beta)(1+\beta)}\right] & \\ & \text{for } 2 \leq \beta < 3, \end{cases} \tag{20}$$

along which the minimum value of y is equal to zero. The maximum value of α_u is given by

$$\alpha_{u,M} = \frac{5}{4} \quad \text{at} \quad \beta = \frac{5+3\sqrt{5}}{4}. \tag{21}$$

In other words, the maximum polydispersity attainable is the same as that for $D \geq 0$. And the lower bound of α for $D < 0$ is determined as follows:

$$\alpha_l = \begin{cases} \dfrac{1}{8}\beta^2 & \text{for} -1 < \beta < \dfrac{20}{7} \\ \dfrac{1}{10}\left[\beta^2 - \beta + 6 + (2-\beta)\sqrt{3(3-\beta)(1+\beta)}\right] & \\ & \text{for } \dfrac{20}{7} \leq \beta < 3. \end{cases} \tag{22}$$

The shape of QCE for $D < 0$ may also be classified into five different patterns, as shown in Figure 2b. To each of these patterns, there corresponds a subregion located within the feasible region of Figure 1b.

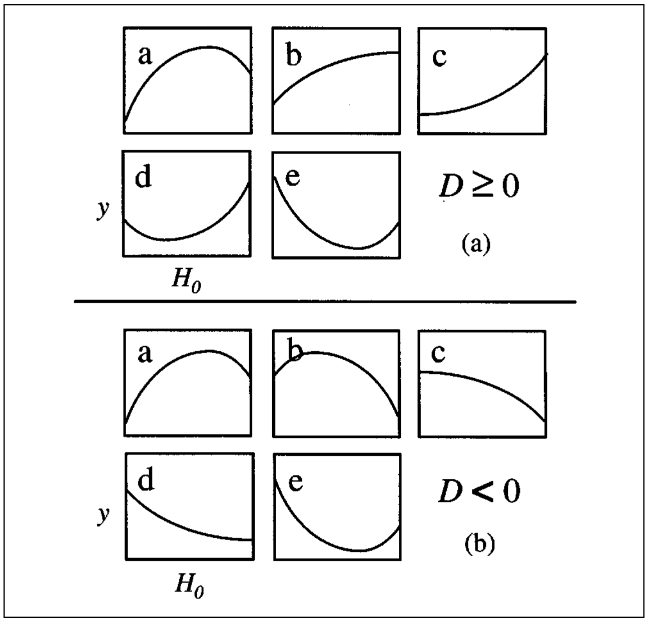

Figure 2. Various patterns for the QCE profiles corresponding to the subregions in Figure 1.

In Figure 1, larger values of α are feasible in subregions d and e for $D \geq 0$ and subregion e for $D < 0$, respectively. From this observation, we see that the polymer product with a larger polydispersity can be obtained by using a QCE with the minimum extremum point between 0 and H_0^*. It is also noticed that the feasible range of α is relatively small in subregions a and b for $D \geq 0$ and in subregions a, b, and c for $D < 0$. This implies that QCE with the maximum extremum point would put a severe restriction on the range of feasible polydispersity.

MWD attainable by QCEs with constraints on the range of y

In practice, the attainable average molecular weights determined in the previous section may lose their physical meaning if the process constraint is not taken into account. For example, the reactor often needs to be operated within a certain temperature range due to process safety or operability. Here we note that the instantaneous degree of polymerization y varies monotonically along with the operating variables such as the reactor temperature, the initiator concentration, and the solvent fraction. Thus, the process constraints can be translated into the appropriate constraints on y.

In this section, we will consider the following transformed constraints; that is, the upper and lower bounds of y:

$$s_1 \leq y(H_0) \leq s_2. \tag{23}$$

These constraints, s_1 and s_2, can be readily identified by performing the reactor-model simulation under the operating conditions close to the process constraints and the attainable number average molecular weight should also be restricted between these two limits; that is, $s_1 \le Y^* \le s_2$. We put s_1 and s_2 into dimensionless form as follows:

$$\delta_1 = \frac{s_1}{Y^*} - 1 \qquad \text{and} \qquad \delta_2 = \frac{s_2}{Y^*} - 1, \tag{24}$$

and thus

$$\delta_2 = \frac{s_2}{s_1}\delta_1 + \left(\frac{s_2}{s_1} - 1\right), \qquad -1 < \delta_1 \le 0 \qquad \text{and} \qquad \delta_2 \ge 0. \tag{25}$$

It is now evident that the attainable polydispersity is restricted not only by the shape of QCEs but also by the values of δ_1 and δ_2.

In the sequel, we shall examine the ranges of the degree of polymerization and the polydispersity attainable by using QCEs under the constrained operating conditions. In this case, the attainable MWD is calculated by the physically realizable pairs of $(\alpha,\ \beta)$ satisfying the following inequalities:

$$\delta_1 \le \beta - \frac{3}{2}[3\beta + 5D]\left(\frac{H_0}{H_0^*}\right) + \frac{15}{4}[\beta + 3D]\left(\frac{H_0}{H_0^*}\right)^2 \le \delta_2 \qquad \text{for} \quad 0 \le H_0 \le H_0^*, \tag{26}$$

in which both the maximum and minimum values of QCEs are required to exist in the constrained range of y, respectively. From Figures 1 and 2, one can easily identify the maximum and minimum values of QCEs. For example, the minimum value of QCE for $D \ge 0$ in Figure 2a is derived as follows:

$$\frac{y_{\min}}{Y^*} = \beta + 1 \qquad \text{at} \quad \frac{H_0}{H_0^*} = 0 \qquad \text{for subregions a, b, and c}$$

$$\frac{y_{\min}}{Y^*} = \beta + 1 - \frac{3(3\beta + 5D)^2}{20(\beta + 3D)} \qquad \text{at} \quad \frac{H_0}{H_0^*} = \frac{3\beta + 5D}{5(\beta + 3D)} \qquad \text{for subregions d and e} \tag{27}$$

and thus the feasible pairs of $(\alpha,\ \beta)$ in the case of the QCE for $D \ge 0$ are required to satisfy the following relation for $y_{\min} \ge s_1$:

$$\beta \ge \delta_1 \qquad \text{for subregions a, b, and c} \tag{28a}$$

$$\alpha \le \frac{1}{10}\left[\beta^2 + \delta_1\beta + 6\delta_1^2 - (2\delta_1 + \beta)\sqrt{3(3\delta_1 + \beta)(\delta_1 - \beta)}\right] \qquad \text{for subregions d and e.} \tag{28b}$$

Also, the maximum value of QCE for $D \ge 0$ can be expressed as follows:

$$\frac{y_{\max}}{Y^*} = \beta + 1 - \frac{3(3\beta + 5D)^2}{20(\beta + 3D)} \qquad \text{at} \quad \frac{H_0}{H_0^*} = \frac{3\beta + 5D}{5(\beta + 3D)} \qquad \text{for subregion a}$$

$$\frac{y_{\max}}{Y^*} = 1 + \frac{1}{4}\beta + \frac{15}{4}D \qquad \text{at} \quad \frac{H_0}{H_0^*} = 1 \qquad \text{for subregions b, c, and d}$$

$$\frac{y_{\max}}{Y^*} = \beta + 1 \qquad \text{at} \quad \frac{H_0}{H_0^*} = 0 \qquad \text{for subregion e,} \tag{29}$$

and, by using Eq. 29 and the inequality condition $y_{\max} \le s_2$, the following inequalities are derived for the feasible pairs of $(\alpha,\ \beta)$ in the case of the QCE for $D \ge 0$:

$$\alpha \ge \frac{1}{10}\left[\beta^2 + \delta_2\beta + 6\delta_2^2 + (2\delta_2 + \beta)\sqrt{3(3\delta_2 + \beta)(\delta_2 - \beta)}\right] \qquad \text{for} \quad \left(\frac{1}{8}\beta^2 \le \alpha < \frac{2}{15}\beta^2\right) \wedge (\beta \le 0) \tag{30a}$$

$$\alpha \le \frac{1}{10}\left[\beta^2 + \delta_2\beta + 6\delta_2^2 - (2\delta_2 + \beta)\sqrt{3(3\delta_2 + \beta)(\delta_2 - \beta)}\right] \qquad \text{for} \quad \left(\frac{2}{15}\beta^2 \le \alpha < \frac{1}{5}\beta^2\right) \wedge (\beta \le 0) \tag{30b}$$

$$\alpha \le \frac{1}{15}\left(2\beta^2 - \delta_2\beta + 2\delta_2^2\right) \qquad \text{for subregions b, c, and d} \tag{30c}$$

$$\beta \le \delta_2 \qquad \text{for subregion e.} \tag{30d}$$

Therefore, the feasible pairs of $(\alpha,\ \beta)$ in the case of the QCE for $D \ge 0$ fall in a region enclosed by Eq. 16 from the constraint on D and Eqs. 28 and 30 from the constraints on the maximum and minimum values of QCE for $D \ge 0$, respectively.

In the same manner, we can derive the realizable pairs of $(\alpha,\ \beta)$ in the case of the QCE for $D < 0$. From the constraint on the minimum value of the QCE for $D < 0$, the following inequality conditions are obtained:

$$\beta \ge \delta_1 \qquad \text{for subregion a} \tag{31a}$$

$$\alpha \le \frac{1}{15}\left(2\beta^2 - \delta_1\beta + 2\delta_1^2\right) \qquad \text{for subregions b, c, and d} \tag{31b}$$

$$\alpha \le \frac{1}{10}\left[\beta^2 + \delta_1\beta + 6\delta_1^2 + (2\beta_1 + \beta)\sqrt{3(3\delta_1 + \beta)(\delta_1 - \beta)}\right] \qquad \text{for} \quad \left(\frac{2}{15}\beta^2 \le \alpha < \frac{1}{5}\beta^2\right) \wedge (\beta \le 0) \tag{31c}$$

$$\alpha \ge \frac{1}{10}\left[\beta^2 + \delta_1\beta + 6\delta_1^2 - (2\delta_1 + \beta)\sqrt{3(3\delta_1 + \beta)(\delta_1 - \beta)}\right] \qquad \text{for} \quad \left(\frac{1}{8}\beta^2 \le \alpha < \frac{2}{15}\beta^2\right) \wedge (\beta \le 0), \tag{31d}$$

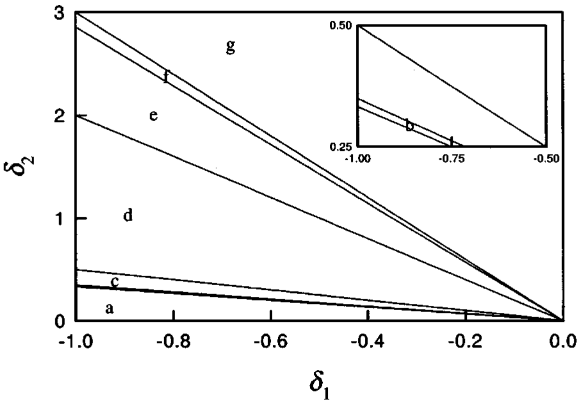

Figure 3. Plane of the constraint parameters (δ_1, δ_2) divided into seven subregions.

δ_1 and δ_2 are defined as $\delta_1 = s_1/Y^* - 1$ and $\delta_2 = s_2/Y^* - 1$, where $s_1 \leq Y^* \leq s_2$. The individual regions of each caption can be represented by the following expressions:

a: $0 \leq \delta_2 < -1/3\delta_1$; b: $-1/3\delta_1 \leq \delta_2 < -7/20\delta_1$; c: $-7/20\delta_1 \leq \delta_2 < -1/2\delta_1$; d: $-1/2\delta_1 \leq \delta_2 < -2\delta_1$; e: $-2\delta_1 \leq \delta_2 < -20/7\delta_1$; f: $-20/7\delta_1 \leq \delta_2 < -3\delta_1$; g: $-3\delta_1 \leq \delta_2$.

and, using the constraint on the maximum value of the QCE for $D < 0$, we can derive the following inequalities:

$$\alpha \leq \frac{1}{10}\left[\beta^2 + \delta_2\beta + 6\delta_2^2 + (2\delta_2 + \beta)\sqrt{3(3\delta_2 + \beta)(\delta_2 - \beta)}\right] \quad \text{for subregions a and b} \qquad (32a)$$

$$\beta \leq \delta_2 \quad \text{for subregions c, d, and e.} \qquad (32b)$$

Therefore, the feasible region for the pairs of (α, β) in the case of the QCE for $D < 0$ is constructed from Eqs. 16, 31, and 32.

In Figure 3, the plane of the constraint parameters, $\{-1 < \delta_1 \leq 0\} \wedge \{0 \leq \delta_2 \leq 3\}$, is divided into seven subregions based on the number of the boundary inequalities enclosing the feasible (α, β) region. To each of these subregions, there is a corresponding particular shape of the feasible region for the pairs of (α, β), as illustrated in Figures 4 and 5. If the constraint parameters fall within the region $\{-1 < \delta_1 \leq 0\} \wedge \{3 < \delta_2\}$, the shape of the feasible (α, β) region is similar to that corresponding to the subregion g in Figure 3.

In each diagram of Figure 4, the boundary consists of several segments. If we begin from the lowest segment passing through the origin and rotate clockwise, the equations to be used successively to construct the segments are listed in sequence in Table 4 by their equation numbers. With respect to Figure 5, the same information is also given in Table 4.

Figures 4 and 5 clearly show the information about the attainable value of $\alpha (= p^*/P - 1)$ within a specific subregion of constraint parameters. For example, we observe that the maximum attainable values of α are identical regardless of the sign of D. Table 5 presents the maximum value of α attainable by the two-step method based on QCEs within a specific subregion of constraint parameters.

Using this information on the attainable average molecular weights, one can efficiently develop the MWD control strategies for producing the desired polymer product. This information will play the central role when on-line modification of the recipe is to be implemented by using the two-step method.

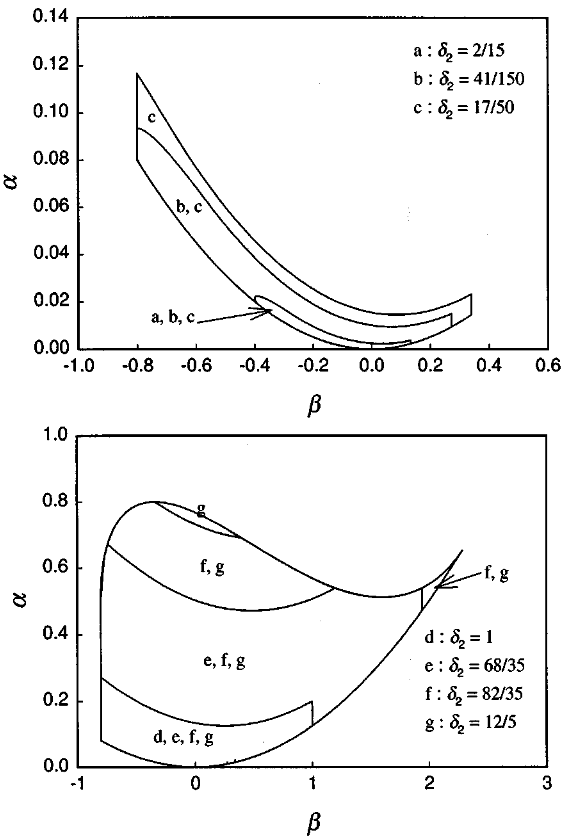

Figure 4. Feasible regions for the pairs of (α, β) corresponding to the subregions in Figure 3 ($\delta_1 = -4/5$) in the case of the QCE for $D \geq 0$.

Application to a Styrene Batch Polymerization Reactor

Variation of y according to the operating condition

Figure 6 shows the variation of y according to the reactor operating conditions such as the reactor temperature and the solvent fraction. In the styrene solution polymerization, y slightly increases with the conversion under the isothermal condition because of the gel effect. Here, two unusual phenomena are observed in the postreaction interval: a rapid decrease or a rapid increase of y by the exhaustion of monomer or initiator, respectively. Figure 7 illustrates these phenomena when generated under the reactor operating conditions corresponding to Figure 6b in terms of the histories of monomer conversion and initiator concentration, respectively. With the high solvent fraction, the level of y is less sensitive to the reactor temperature and remains low in comparison to the case of the low solvent fraction.

Estimation of the attainable MWD

The following example illustrates the ideas described earlier, demonstrating the two-step method based on QCEs. The specific operating condition considered here is the same as

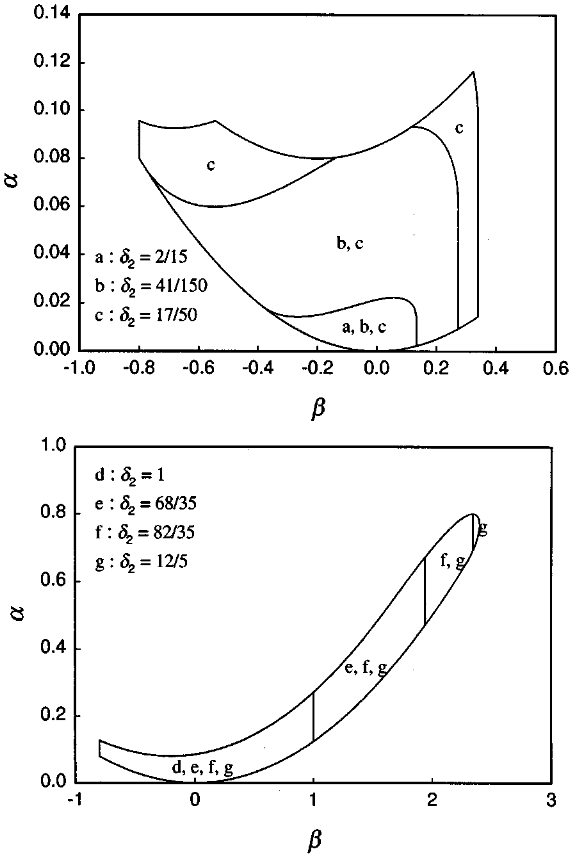

Figure 5. Feasible regions for the pairs of $(\alpha,\ \beta)$ corresponding to the subregions in Figure 3 $(\delta_1 = -4/5)$ in the case of the QCE for $D < 0$.

Table 4. Equations to be Used Successively for the Construction of Feasible $(\alpha,\ \beta)$ Regions

	Figure 4	Figure 5
a	16, 30a, 30b, 30c, 30d	16, 32a, 32b
b	16, 30a, 28a, 30b, 30c, 30d	16, 32a, 31b, 32a, 32b
c	16, 28a, 30b, 30c, 30d	16, 31a, 32a, 31b, 32a, 32b
d	16, 28a, 30c, 30d	16, 31a, 31b, 32b
e	16, 28a, 28b, 30c, 28b, 30d	16, 31a, 31b, 31c, 32b
f	16, 28a, 28b, 30c, 28b	16, 31a, 31b, 31c, 32b, 31d
g	16, 28a, 28b	16, 31a, 31b, 31c, 31d

that in Figure 6b: the reactor temperature constrained between 50°C and 90°C, the initial initiator concentration 0.03 mol/L, and the solvent fraction 0.25. Using the results of model simulation at 50°C and 90°C, respectively, we assign the constraints on y as $s_1 = 190$ and $s_2 = 590$. Hence we consider the value of Y^* between 190 and 590. Then the following linear relation exists between δ_1 and δ_2:

$$\delta_2 = \frac{59}{19}\delta_1 + \frac{40}{19} \qquad \text{for} \quad -\frac{40}{59} < \delta_1 \leq 0.$$

We also set the value of p in Eq. 13 equal to 1.7 by considering the results of the reactor-model simulation under various isothermal conditions. Using the maximum attainable values of α given in Table 5, we plot the feasible region of the MWD objective specified by Y^* and P^* in Figure 8. Note that the feasible region of the MWD objective is identical regardless of the sign of D, and the range of the attainable polydispersity varies depending on the desired degree of polymerization. In this example, a large polydispersity is attainable at the degree of polymerization around 300.

Calculation of the recipes for the reactor temperature

In this example, we set the desired degree of polymerization Y^* equal to 250, which corresponds to $\delta_1 = -6/25$ and $\delta_2 = 34/25$. Figure 9 shows the feasible $(\alpha,\ \beta)$ regions when the QCEs are applied to these constraint parameters. First, the attainable range of the polydispersity at $Y^* = 250$ in Figure 8 is given by $1.7 \leq P^* \leq 1.8224$. Thus we set P^* and X^*

Table 5. Maximun Value of α Attainable by the Two-Step Method Based on QCEs

Condition on δ_1 and δ_2	Maximum Value of α Attainable, α_M	Value of β Corresponding to α_M	
		$D \geq 0$	$D < 0$
$\delta_1 < -\left(\frac{5+3\sqrt{5}}{4}\right)\delta_2$	$\alpha_M = \frac{5}{4}\delta_2^2$	$\beta = -\left(\frac{5+3\sqrt{5}}{4}\right)\delta_2$	$\beta = -\left(\frac{5-3\sqrt{5}}{4}\right)\delta_2$
$-\left(\frac{5+3\sqrt{5}}{4}\right)\delta_2 \leq \delta_1 < -2\delta_2$	$\alpha_M = \frac{1}{10}[\delta_1^2 + \delta_1\delta_2 + 6\delta_2^2 - (\delta_1 + 2\delta_2)\sqrt{3(\delta_1 + 3\delta_2)(\delta_2 - \delta_1)}]$	$\beta = \delta_1$	$\beta = -\frac{1}{2}[\delta_1 + 3\delta_2 - \sqrt{3(\delta_1 + 3\delta_2)(\delta_2 - \delta_1)}]$
$-2\delta_2 \leq \delta_1 < -\frac{1}{2}\delta_2$	$\alpha_M = \frac{1}{15}(2\delta_1^2 - \delta_1\delta_2 + 2\delta_2^2)$	$\beta = \delta_1$	$\beta = \delta_2$
$-\frac{1}{2}\delta_2 \leq \delta_1 < \left(\frac{5-3\sqrt{5}}{5}\right)\delta_2$	$\alpha_M = \frac{1}{10}[6\delta_1^2 + \delta_1\delta_2 + \delta_2^2 + (2\delta_1 + \delta_2)\sqrt{3(3\delta_1 + \delta_2)(\delta_1 - \delta_2)}]$	$\beta = -\frac{1}{2}[3\delta_1 + \delta_2 + \sqrt{3(3\delta_1 + \delta_2)(\delta_1 - \delta_2)}]$	$\beta = \delta_2$
$\left(\frac{5-3\sqrt{5}}{5}\right)\delta_2 \leq \delta_1$	$\alpha_M = \frac{5}{4}\delta_1^2$	$\beta = -\left(\frac{5-3\sqrt{5}}{4}\right)\delta_1$	$\beta = -\left(\frac{5+3\sqrt{5}}{4}\right)\delta_1$

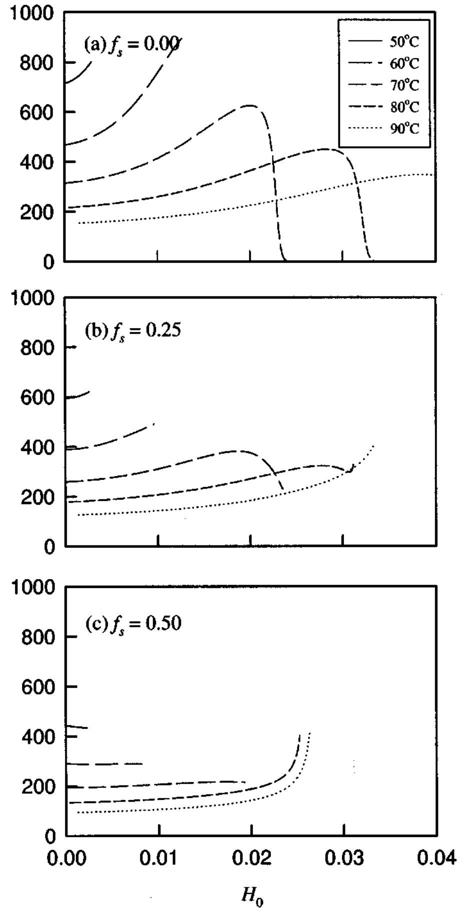

Figure 6. Variation of y for three different solvent fractions under various isothermal conditions: $I(0) = 0.03$ mol/L.

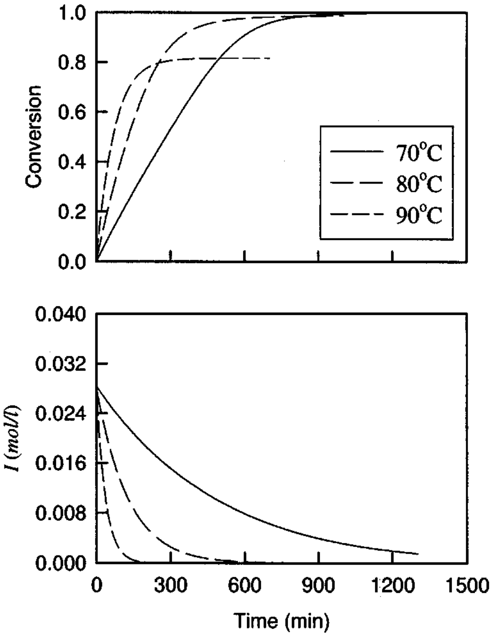

Figure 7. Histories of monomer conversion and initiator concentration under the reactor operating condition corresponding to Figure 6b.

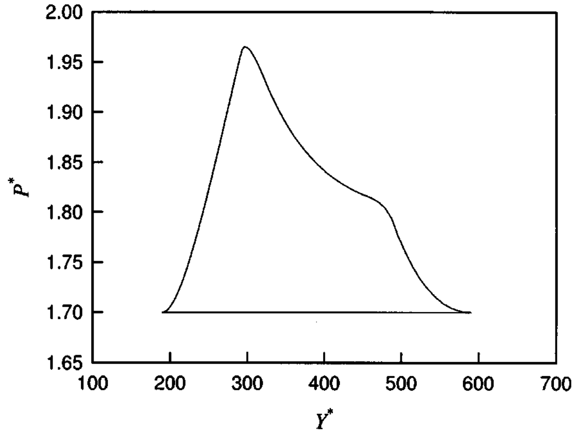

Figure 8. Feasible region of the MWD objective attainable by the two-step method based on QCEs under the reactor operating condition corresponding to Figure 6b.

to 1.8 and 0.5, respectively. One can read the range of β from Figure 9 and obtain the feasible range of $y(0)$ as $193.3 \leq y(0) \leq 292.7$ for $D \geq 0$ and $392.7 \leq y(0) \leq 421.5$ for $D < 0$. Then we can calculate a set of the temperature recipes to produce the polymer satisfying the MWD specification by choosing the initial reactor temperature within the feasible range of $y(0)$.

Finally, we calculate the temperature recipes by setting the initial reactor temperatures to 67.5, 73.0, and 78.5°C for $D \geq 0$ and 59°C for $D < 0$. Figure 10 shows the calculated temperature trajectories located between the temperature constraints

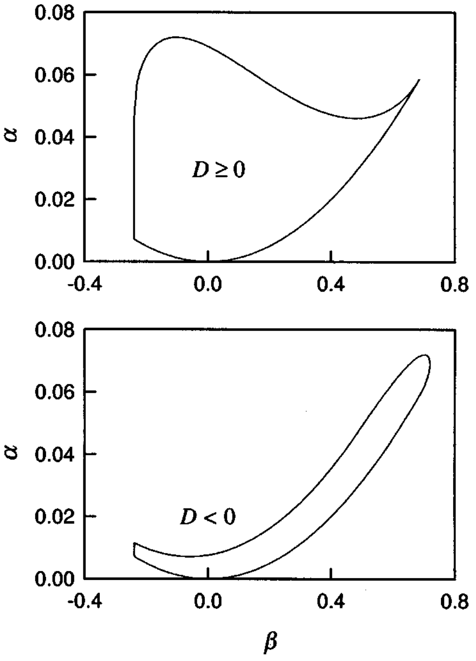

Figure 9. Feasible regions for the pairs of (α, β) with the constraint parameters $\delta_1 = -6/25$ and $\delta_2 = 34/25$ under the reactor operating condition corresponding to Figure 6b.

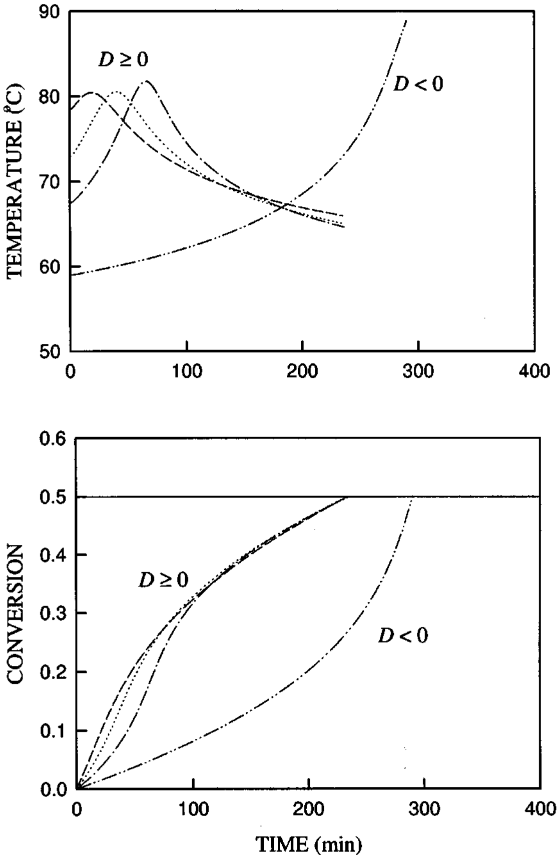

Figure 10. Reactor temperature trajectories that would produce the polymer satisfying the MWD objective $Y^* = 250$ and $P^* = 1.8$, and the histories of the monomer conversion corresponds to the reactor temperature trajectories.

The reactor operating condition corresponds to Figure 6b.

and the histories of the monomer conversion. The operation time is about 235 min for the three trajectories with $D \geq 0$ and 290 min for the trajectory with $D < 0$. Thus, if we prefer to reduce the batch time with the given MWD specification, it is natural to choose a temperature trajectory with $D \geq 0$. The shape of the temperature trajectory is the bell type, with the maximum at the first half for $D \geq 0$, whereas it is the increasing type for $D < 0$. To select an operating recipe, we need to consider the performance of the given control system. For example, if the reactor cooling is rather difficult, one may select the temperature trajectory for $D < 0$ despite the longer batch time.

Figure 11 contains the histories of the degree of polymerization and the polydispersity. For the three trajectories with $D \geq 0$, these histories coincided with one another at the latter part of the course of the reaction. In all four cases, one can clearly see that the MWD specification is satisfied at the desired final conversion level.

In this example, the feasible ranges of $y(0)$ turn out to be somewhat conservative due to the fact that the lower constraint on y, s_1, is rather severe. For instance, the maximum temperatures for $D \geq 0$ in Figure 10 are found to be about 80°C, which corresponds to $s_1 = 190$ at low conversion. To improve this conservativeness in the case of $D \geq 0$, one may lower s_1, taking the fact that the maximum temperature is formed at low conversion into consideration.

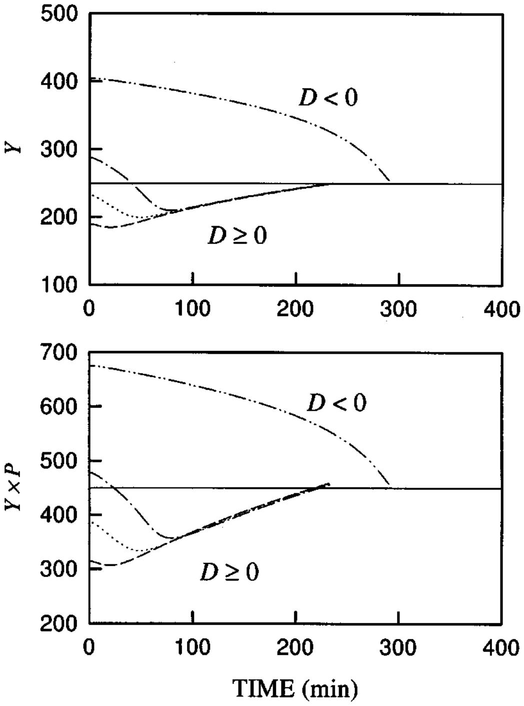

Figure 11. Histories of the degree of polymerization and polydispersity corresponding to the reactor temperature trajectories in Figure 10.

Summary and Concluding Remarks

Here, we investigated the molecular-weight distribution attainable in a batch free-radical polymerization reactor in association with the two-step method. The MWD was specified by the degree of polymerization and the polydispersity. The problem was analytically solved under some assumptions, on which the two-step method is based. Furthermore, the entire computational procedure was intelligently organized by virtue of the fact that the appropriate initial operating condition and the shape of the temperature trajectory can be selected based on the preliminary analysis of the attainable MWD. As a result, the actual computational load is very low compared to the conventional optimization methods and the original two-step method. In addition, the problem involved with constraints on the operating condition is analytically treated.

The current version of the two-step method was applied to the styrene polymerization reactor. We illustrated the attainable MWD under a specific operating condition with constraints; calculated various reactor temperature trajectories to produce the desired polymer product; and demonstrated that the temperature trajectories indeed gave rise to the polymer product with the desired MWD specification at the desired final conversion level.

The ability to visualize the attainable MWD will allow an engineer how to easily design the recipes that meet the desired MWD objectives. For the on-line two-step method, the information on the attainable MWD is essential so that the feasibility of the target MWD can be inspected and the trajectory intelligently adjusted in order to compensate for the process disturbances at every time step.

In this study, we have applied the two-step method based on the quadratic y profile. However, the quadratic y profiles are only the subset of $y(H_0)$ trajectories that can be used as the constitutive equations for the two-step method. It is obvious that we need to explore the y profile in a more general way and estimate the attainable MWD on the basis of such a y profile.

Acknowledgments

This work was supported by the Korea Science and Engineering Foundation (KOSEF) through the Automation Research Center at Pohang University of Science and Technology.

Notation

f = initiator efficiency
F_k = kth moment of dead polymer concentration ($k = 0, 1, 2$), mol/L
G_k = kth moment of living polymer concentration ($k = 0, 1, 2$), mol/L
H_k = kth moment of total polymer concentration ($k = 0, 1, 2$), mol/L
I = initiator or its concentration, mol/L
k = reaction rate constant, s^{-1} or L/(mol·s)
M = monomer or its concentration, mol/L
P_n = dead polymer of chain length n or its concentration, mol/L
R_n = living polymer of chain length n or its concentration, mol/L
S = solvent or its concentration, mol/L
W = molecular weight, g/mol
x = fractional monomer conversion
ρ = density, g/L

Subscripts

d = initiator decomposition
m = monomer
p = propagation or polymer
s = solvent (toluene)
t = termination
tc = termination by combination
td = termination by disproportionation
trm = chain transfer to monomer
trs = chain transfer to solvent

Literature Cited

Ahn, S. M., S. C. Chang, and H.-K. Rhee, "Application of Optimal Temperature Trajectory to Batch PMMA Polymerization Reactor," *J. Appl. Poly. Sci.*, **69**, 59 (1998).

Chang, J. S., and J. L. Lai, "Computation of Optimal Temperature Policy for Molecular Weight Control in a Batch Polymerization Reactor," *Ind. Eng. Chem. Res.*, **31**, 861 (1992).

Chen, S. A., and W. F. Jeng, "Minimum End Time Policies for Batchwise Radical Chain Polymerization," *Chem. Eng. Sci.*, **33**, 735 (1978).

Duerksen, J. H., A. E. Hamielec, and J. W. Hodgins, "Polymer Reactors and Molecular Weight Distribution: I. Free Radical Polymerization in a Continuous Stirred-Tank Reactor," *AIChE J.*, **13**, 1081 (1967).

Hamer, J. W., T. A. Akarmov, and W. H. Ray, "The Dynamic Behavior of Continuous Polymerization: II. Nonisothermal Solution Homopolymerization and Copolymerization in a CSTR," *Chem. Eng. Sci.*, **36**, 1897 (1981).

Hicks, J., A. Mohan, and W. H. Ray, "The Optimal Control of Polymerization Reactors," *Can. J. Chem. Eng.*, **47**, 590 (1969).

Nunes, R. W., J. R. Martin, and J. F. Johnson, "Influence of Molecular Weight and Molecular Weight Distribution on Mechanical Properties of Polymers," *Poly. Eng. Sci.*, **22**, 205 (1982).

Ponnuswamy, S. R., S. L. Shah, and C. A. Kiparissides, "Computer Optimal Control of Batch Polymerization Reactor," *Ind. Eng. Chem. Res.*, **26**, 2229 (1987).

Sacks, M. E., and J. A. Bisenberger, "Optimization Policies for Batch Chain Addition Polymerization," *Chem. Eng. Sci.*, **36**, 1401 (1981).

Schuler, H., and Z. Suzhen, "Real-Time Estimation of the Chain Length Distribution in a Polymerization Reactor," *Chem. Eng. Sci.*, **40**, 1891 (1985).

Tadmor, Z., and C. G. Gogos, *Principles of Polymer Processing*, Wiley, New York (1979).

Takamatsu, T., S. Shioya, and Y. Okada, "Molecular Weight Distribution Control in a Batch Polymerization Reactor," *Ind. Eng. Chem. Res.*, **27**, 93 (1988).

Thomas, I. M., and C. Kiparissides, "Computation of the Near-Optimal Policies for a Batch Polymerization Reactor," *Can. J. Chem. Eng.*, **62**, 284 (1984).

Yoo, K. Y., B.-G. Jeong, and H.-K. Rhee, "Molecular Weight Distribution Control in a Batch Polymerization Reactor Using the On-line Two-step Method," *AIChE Meeting*, Miami (1998).

Manuscript received Sept. 30, 1998, and revision received Mar. 19, 1999.